Int J Thermophys (2013) 34:1953–1961
DOI 10.1007/s10765-013-1502-3

Contribution to the Transient Plane Source Method for Measuring Thermophysical Properties of Solids

Svetozár Malinarič

Received: 29 April 2013 / Accepted: 13 August 2013 / Published online: 27 August 2013

Abstract The transient plane source method of measuring the thermal conductivity and thermal diffusivity uses a sensor in the shape of a thin disk, which simultaneously serves as the heat source and thermometer. This study describes improvements of the experimental apparatus, providing some details of the electrical bridge with the aim to obtain maximum reliability of the measurement results. The aim of the temperature function analysis is to find the optimal time of measurement. The relation between the data time window used for fitting, the uncertainty of the sensor temperature measurement, and the uncertainty of the results is presented and graphically illustrated using numerical simulation of the experiment. The theory was confirmed by the evaluation of real measurements on polymethylmetacrylate. The temperature function analysis revealed that a decrease of the temperature measurement uncertainty need not always lead to a fall in the total uncertainty of the results but to shorter experiments and smaller specimens.

Keywords Polymethylmetacrylate · Temperature function analysis · Thermal conductivity · Thermal diffusivity · Transient plane source method

1 Introduction

Transient methods [1] for measuring the thermophysical properties of materials are characterized by the heat source and thermometer placed inside the specimen. This arrangement suppresses the influence of the specimen surface on the measuring process. The theoretical model is described by a temperature function, which is a

Svetozár Malinarič (✉)
Department of Physics, Constantine the Philosopher University,
Trieda Andreja Hlinku 1, 94974 Nitra, Slovak Republic
e-mail: smalinaric@ukf.sk

solution of the heat equation with boundary and initial conditions corresponding to the experimental arrangement. The experiment consists of measuring the temperature response to the input heat flux with a steady-state initial condition. The evaluation is based on determining the thermal conductivity and thermal diffusivity by fitting the temperature function to the temperature response.

The transient plane source [2] (TPS) method uses a one-sensor system, where the heat source simultaneously serves as the thermometer. The sensor, in the shape of a thin disk, is placed between two sample pieces. Heat is produced by the passage of an electrical current, in the form of a stepwise function, through the sensor, the temperature of which is determined by measuring its electrical resistance. The sensor is completely surrounded by the specimen, and in the time window used for calculation, the heat flow must not reach the free surface of the specimen.

The aim of this study is to improve the experimental arrangement and analyze the influence of the temperature measurement uncertainty and the data time window used for calculation on the uncertainty of determination of the thermophysical parameters of the specimen.

2 Theoretical Model

The theoretical model of the TPS method is created by the following conditions:

(i) The sensor consists of concentric and equally spaced circular line sources.
(ii) The thickness and heat capacity of the sensor are negligible.
(iii) There is no thermal resistance between the sensor and specimen.
(iv) The specimen is infinite in all directions.
(v) The input power in the sensor is stepwise.

The mean temperature increase of the sensor (temperature function) is given by [2]

$$T(\tau) = \frac{P}{\pi^{3/2} r \lambda} D_n(\tau), \tag{1}$$

where P is the input heat power, r is the radius of the sensor, $\tau = \sqrt{t/\theta}$, $\theta = r^2/a$ is the characteristic time, and t is the real time of the experiment. λ and a are the thermal conductivity and thermal diffusivity of the specimen, respectively. The shape function has the form,

$$D_n(\tau) = [n(n+1)]^{-2} \int_0^{\tau} \frac{\mathrm{d}s}{s^2} \sum_{l=1}^{n} l \sum_{k=1}^{n} k \exp\left(-\frac{l^2+k^2}{4n^2 s^2}\right) I_0\left(\frac{lk}{2n^2 s^2}\right), \tag{2}$$

where n is the number of circular line sources and I_0 is the modified Bessel function. For a very large number of rings, the shape function tends toward

$$D_\infty(\tau) = \int_0^{\tau} \frac{\mathrm{d}s}{s^2} \int_0^{1} v\,\mathrm{d}v \int_0^{1} u\,\mathrm{d}u \exp\left(-\frac{u^2+v^2}{4s^2}\right) I_0\left(\frac{uv}{2s^2}\right) \tag{3}$$

The numerical calculation of $D_n(\tau)$ and $D_\infty(\tau)$ is not possible for $\tau < 0.03$ [3], so it is necessary to estimate the shape functions in this interval by a polynomial as

$$D(\tau) = A + B\tau + C\tau^2. \tag{4}$$

For $t \to 0$ the model corresponds to one-dimensional heat flow into an infinite medium [4] with the following temperature function:

$$T(\tau) = \frac{q}{\lambda}\sqrt{\frac{at}{\pi}} = \frac{P}{\pi^{3/2} r\lambda}\tau, \tag{5}$$

where q is the power per unit area dissipated by the sensor. Connecting Eqs. 1, 4, and 5, we have $A = 0$ and $B = 1$. The last coefficient $C = -0.570$ is estimated by comparing the first derivative of Eqs. 3 and 4 at point $\tau = 0.03$.

3 Experiment

The increase of the sensor resistance should be measured by using a digital voltmeter and a bridge as described in [5]. In this paper a new experimental arrangement for measurement at the laboratory temperature is designed, which removed some sources of the measurement uncertainty of the bridge in [5]. It is based on a two-channel nanovoltmeter (Keithley 2182A) as illustrated in Fig. 1. The main advantage of the circuit lies in two modes of measurement, which increases the reliability of the results. In a comparative mode the voltmeter simultaneously measures the voltages U_1 and U_2. This mode suppresses the influence of the constant voltage source instability and eliminates the resistance of the sensor leads from the calculation. Then the sensor resistance is determined from the following formula:

$$R = R_\mathrm{c}\frac{U_1}{U_2}, \tag{6}$$

where R_c is the constant power resistor. In the bridge mode the voltmeter measures the voltage across the bridge u_1 during the transient and, afterward, it measures the voltage of the source u_2 before the heating current is turned off. This mode enables use of the lowest voltage range, which will result in better measurement accuracy. A single-channel measurement enables a higher sampling frequency and, consequently, measurements on materials with a high thermal diffusivity. The sensor resistance can be calculated as follows:

$$U_a = u_2\frac{R_a}{R_a + R_b} \quad U_b = u_2 - U_a \quad R = (R_\mathrm{c} + R_l)\frac{U_a + u_1}{U_b - u_1} - R_l, \tag{7}$$

where R_a, R_b, R_c are constant resistors and R_l is the resistance of one sensor lead.

The other advantages of the bridge in Fig. 1 are as follows.

1. Measuring at the laboratory temperature only, the resistance of the sensor changes less than 3 %. So the value of the constant resistor R_c can be set close to the sensor

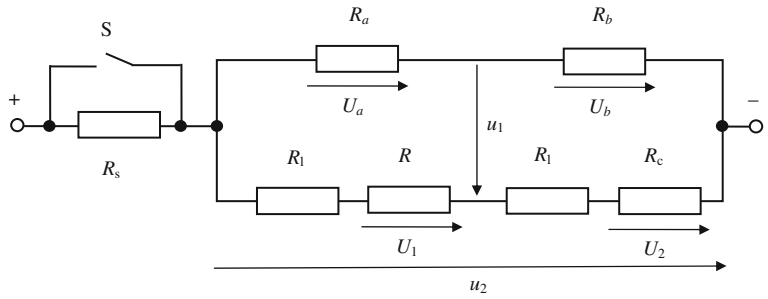

Fig. 1 Bridge for sensor resistance R measurement using two-channel nanovoltmeter. U_1, U_2 are measured voltages in comparative mode and u_1, u_2 are measured voltages in bridge mode. S is the switch for starting the experiment

resistance R. This is necessary for keeping the power input constant during the measurement [5].

2. The instability introduced by the potentiometer is removed by replacing it with two constant resistors.
3. There is no need to balance the bridge, which is still slightly unbalanced, $R \approx R_c$, $R_a \approx R_b$, keeping the voltage across the bridge u_1 within the lowest range, 10 mV.
4. The resistance of the sensor R is measured, not only its increase as in [5]. This provides more information of the experiment.
5. The sensor leads are placed into adjacent arms of the bridge, which will suppress changes of the leads' resistance caused by variations in temperature.
6. Inserting the series resistor $R_s \approx 200R$ enables measurement of the sensor resistance before the heating current is turned on. The heating effect is negligible but the steady state can be monitored before the start of the experiment. A sensor temperature stability better than 1 mK over an interval of 60 s was reached.

In [5], the probing depth is defined as a measure of how far into the specimen the heat flows during the time window used for calculation and is given by

$$p = 2\sqrt{at_{\max}} = 2r\sqrt{\frac{t_{\max}}{\theta}}, \tag{8}$$

where $t_{\max}$ is the maximum time of this window. The specimen size can be determined using recommendation 6.1.3 in [5] which says that the distance x from any part of the sensor to any part of the outside boundary of the specimen should be larger than the sensor radius. And an increase in this distance beyond the size of the specimen diameter does not improve the accuracy of the results. This can be expressed as

$$r < x < 2r, \tag{9}$$

and considering Eq. 8, we have the condition for duration of the measurement as

$$\frac{\theta}{4} < t_{\max} < \theta \tag{10}$$

The estimates of the thermophysical parameters a and λ are determined by fitting predicted values of the sensor resistance given by

$$R(t) = R_0 + \frac{\alpha\ R_0 P}{\pi^{3/2} r \lambda} D_n \left(\frac{\sqrt{a\,(t - t_c)}}{r} \right) \tag{11}$$

to the measured points $[t_i, R_i]$. α is the temperature coefficient of resistivity of the sensor (Ni), P is the input heat power, r is the radius of the sensor, and D_n is the shape function defined by Eq. 2. The thermal diffusivity a and time correction t_c [5] will be iterated until the correlation coefficient of the dependence R_i versus $D_n(t_i)$ reaches its maximum. Finally, R_0 is determined from the intercept and λ from the slope of this line.

4 Temperature Function Analysis

Assume the temperature function in Eq. 1 is of a known analytical form,

$$T(t, \vec{\alpha}) = T(t, \alpha_1, \alpha_2, \ldots \alpha_p), \tag{12}$$

where the time t is a variable and $\vec{\alpha}$ is a vector of unknown parameters. The sensitivity coefficient defined by [6]

$$\beta_j(t, \vec{\alpha}) = \alpha_j \frac{\partial T(t, \vec{\alpha})}{\partial \alpha_j} \tag{13}$$

is a measure of the change in the temperature function due to the variation of the estimated parameter. The sensitivity coefficients should be analyzed because it is not possible to determine the parameters if their sensitivity coefficients are small or linearly dependent on each other. However, it is difficult to judge the linear dependence and such an analysis has only a qualitative nature. The quantitative access to this problem involves determination of the uncertainty of the thermophysical parameter estimates. In this analysis, no deviations between the experiment and theoretical model are considered. The temperature measurement uncertainty is assumed to be the only source of uncertainty of the results. Then the standard uncertainty of the least-squares estimate of the parameter α_j is given by [7–9]

$$u^2(\alpha_j) = \left\{ (\boldsymbol{X}^T \cdot \boldsymbol{X})^{-1} \right\}_{jj} u^2(T) = A^2(\alpha_j)\, u^2(T), \tag{14}$$

where $u(T)$ is the standard uncertainty of the temperature measurement and $\boldsymbol{X}$ is the sensitivity matrix defined by

$$\{X_{ij}\} = \frac{\partial T(t_i, \vec{a})}{\partial \alpha_j} \tag{15}$$

According to Eq. 14, the uncertainty of the parameter estimates consists of two components. The first, here referred to as the uncertainty coefficient $A(\alpha_j)$, is given by the temperature function and selection of measured points. The second is the temperature measurement uncertainty. So we have a simple relation between the data time window, connected with the duration of the measurement, and the uncertainty of the results. It should be emphasized that the uncertainties in this analysis do not include any systematic effects and the temperature measurement uncertainty caused by random noise can be determined as the standard deviation of residuals.

The aim of the following analysis consists in determining the time window necessary for obtaining the required value of the thermophysical parameter uncertainty. The easiest way is via numerical simulation of the experiment. We take the parameters of the polymeric material $\lambda = 0.2\,\mathrm{W}\cdot\mathrm{m}^{-1}\cdot\mathrm{K}^{-1}$, $a = 0.1\,\mathrm{mm}^2\cdot\mathrm{s}^{-1}$, sensor radius $r = 6.4\,\mathrm{mm}$, and heating power $P = 0.02\,\mathrm{W}$, which causes a temperature increase of about 1.5 K. We use the temperature function,

$$T(t) = T_0 + \frac{P}{\pi^{3/2} r \lambda} D_\infty \left(\frac{\sqrt{a\,(t - t_\mathrm{c})}}{r} \right) \tag{16}$$

and compute the coefficients $A(\alpha_j)$ from Eq. 14 for a sampling period $\Delta = 0.4\,\mathrm{s}$ and a total number of samples of 1000. The time window used for calculation will be $(t_b,\ t_b + t_\mathrm{s})$, where $t_b = 20\,\mathrm{s}$ represents the deviating points at the beginning of the experiment [5] and t_s is the size of the window. T_0 and t_c are nuisance unknown parameters. The first corresponds to the initial sensor temperature plus the increase in temperature over the insulating layers of the sensor, and the second to the small time delay between the start of the input heat power and the start of the voltmeter sampling. The relative standard uncertainty of the parameter estimate can be determined from

$$u^+(\alpha_j) = \frac{u(\alpha_j)}{\alpha_j} = \frac{A(\alpha_j)}{\alpha_j} u(T) = A^+(\alpha_j) u(T), \tag{17}$$

where $A^+(\alpha_j)$ is the relative value of the uncertainty coefficient. Figure 2 shows the results of numerical simulation. The computed relative coefficients are plotted on a logarithmic scale against the size of the time window t_s in nondimensional scale. A_3^+ is the coefficient computed with three unknown parameters a, λ, and T_0 while the time correction t_c is set to zero. A_4^+ is the coefficient computed with all four parameters as unknowns. The decrease of all four curves in Fig. 2 can be interpreted as the larger is the time of measurement, the smaller is the uncertainty of the results. We can also see that the uncertainty of parameter a will be considerably larger than that of parameter λ, and more unknown parameters will cause a larger uncertainty of the results.

Figure 3 illustrates the influence of the experimental parameters on the measurement results. Curve (a) corresponds to the original parameters, $P = 0.02\,\mathrm{W}$, $t_b = 20\,\mathrm{s}$, and $\Delta = 0.4\,\mathrm{s}$. Each of other curves was computed with one of the parameters changed to half of its original value. All curves seem to have the same shape shifted in the ordinate direction. As expected, the influence of the amount of the data omitted at the beginning of the transient t_b and the square root of the sampling period Δ are directly proportional while the influence of the heating power P is inversely proportional.

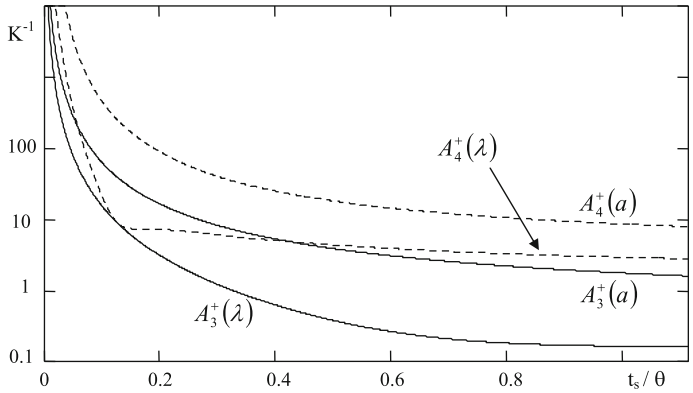

Fig. 2 Relative uncertainty coefficients of the parameters a and λ, computed for 3 and 4 unknown parameters versus the size of the time window t_s in nondimensional scale

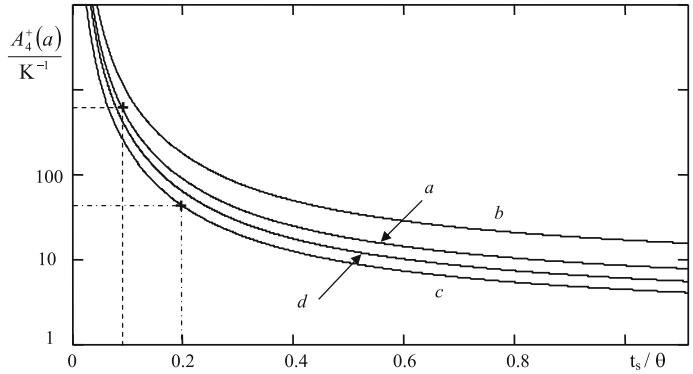

Fig. 3 Relative coefficient $A_4^+(a)$ versus the size of the time window t_s in nondimensional scale for various parameters of the experiment: (a) as in Fig. 2, (b) $P = 0.01$ W, (c) $t_b = 10$ s, and (d) $\Delta = 0.2$ s

5 Results and Discussion

The measurements were performed at the laboratory temperature by using the sensor Hot Disk AB Type 5501 with a number of rings of 16, a radius of 6.4 mm, a resistance of about 13 Ω, and a temperature coefficient of resistivity of 0.0048 K^{-1}. The specimens made from polymethylmetacrylate (PMMA) had a cylindrical shape with a diameter of 30 mm and a thickness of 9 mm. The characteristic time $\theta = 350$ s and $t_{max} > \theta/4 = 88$ s; so, the time of the measurement was set to 120 s which means 300 samples with a sampling period $\Delta = 0.4$ s. The measurements were performed in both bridge and comparative modes. The standard deviation of residuals and the beginning of the time window used for calculation t_b were determined from the time dependence of the residuals as illustrated in Fig. 4 and presented in Table 1.

The previous two experiments were used to verify the theory described in Sect. 4. The procedure is illustrated in Table 1. First, the relative coefficient A_4^+ is determined using Eq. 17 for a required value of 1 % of the relative uncertainty of the parameter a. This value can be regarded as the reasonable lower limit for thermophysical parameter

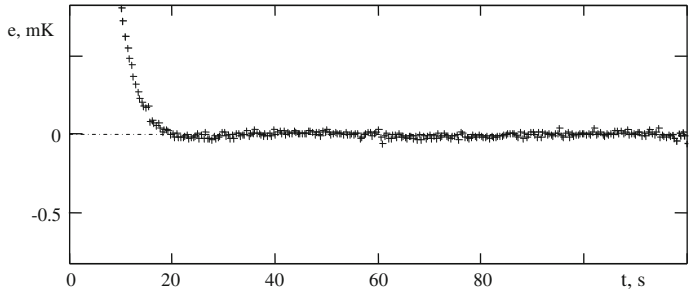

Fig. 4 Time dependence of residuals measured in bridge mode with heating power of 20 mW

Table 1 Measurement evaluation using the time window designed for 1 % uncertainty of the results

Mode	$u(T)$ (mK)	$A_4^+(a)$ (K^{-1})	$t_b(s)$	$\frac{t_s}{\theta}$	$t_s(s)$	$\lambda(W \cdot m^{-1} \cdot K^{-1})$	$a(mm^2 \cdot s^{-1})$
Bridge	0.016	630	20	0.09	30	0.205	0.121
Comparative	0.20	50	10	0.2	68	0.205	0.124

Table 2 Results of the measurements on PMMA using all measured data

	$\lambda(W \cdot m^{-1} \cdot K^{-1})$	$a(mm^2 \cdot s^{-1})$
Arithmetic mean	0.206	0.122
Standard deviation	0.001	0.002
Coefficient of variation	0.5 %	1.6 %

measurements considering the other sources of uncertainty, above all, the deviations between the model and experiment. Second, the size of the window is determined as seen in Fig. 3, for the bridge mode marked as dashed line and for the comparative mode marked as dashed–dotted line. Finally, both thermophysical parameters are computed by fitting in this time window.

Table 2 shows the results of 20 measurements made in comparative and bridge modes with the heating power set to values from 20 mW to 100 mW at a laboratory temperature from 20 °C to 23 °C. The apparatus was disassembled and reassembled before each measurement. All measured data were used for fitting, so $t_b + t_s = 120$ s. The results of thermophysical parameters in Tables 1 and 2 are equivalent; so, we showed that the time windows determined in Table 1 are sufficient for calculation of the parameters. The real uncertainty of the results will be higher than the values in Table 2 because of the deviations between the model and experiment and other systematic errors. However, an increase in the time of measurement does not improve the total uncertainty of the results and measuring beyond the values presented in Table 1 is a waste of time and specimen material.

6 Summary

The first part of this study describes improvements of the experimental apparatus giving some details of the electrical bridge with the aim to obtain maximum reliability

of the measurement results. The second is devoted to temperature function analysis and to finding the optimal time of measurement. The relation between the data time window used for fitting, the uncertainty of the sensor temperature measurement, and the uncertainty of the results was presented and graphically illustrated. In real measurements on PMMA, temperature function analysis was used to determine the time window required for a relative uncertainty of the results better than 1 %. Finally, we showed that this window was sufficient for estimation of thermophysical parameters.

The improvements in the instrument caused a decrease of the temperature measurement uncertainty which need not always lead to a fall in the total uncertainty of the results because of the other sources. However, the temperature function analysis showed that it leads to the use of a smaller time window resulting in a shorter time of the measurement and smaller specimens.

References

1. Ľ. Kubičár, V. Boháč, in *Proceedings of 24th International Conference on Thermal Conductivity/12th International Thermal Expansion Symposium*, ed. by P.S. Gaal, D.E. Apostolescu (Technomic Pub., Lancaster, PA, 1999), p. 135
2. S.E. Gustafsson, Rev. Sci. Instrum. **62**, 797 (1991)
3. Y. Jannot, Z. Acem, Meas. Sci. Technol. **18**, 1229 (2007)
4. E. Karawacki, B.M. Suleiman, I. ul-Haq, B. Nhi, Rev. Sci. Instrum. **63**, 4390 (1992)
5. ISO, *Plastics—Determination of Thermal Conductivity and Thermal Diffusivity—Part 2*. ISO 22007-2 (ISO, Geneva, 2008)
6. V. Boháč, M.K. Gustavsson, Ľ. Kubičár, S.E. Gustafsson, Rev. Sci. Instrum. **71**, 2452 (2000)
7. J.V. Beck, K.J. Arnold, *Parameter Estimation in Engineering and Science* (Wiley, New York, 1977)
8. S. Malinarič, P. Dufíšek, Acta Phys. Slovaca **55**, 165 (2005)
9. S. Malinarič, Int. J. Thermophys. **28**, 20 (2007)